THE PUBLISHING HOUSE
OF THE ROMANIAN ACADEMY

PROCEEDINGS OF THE ROMANIAN ACADEMY, Series A,
Volume 25, Number 2/2024, pp. 139–146
DOI: 10.59277/PRA-SER.A.25.2.08

MORPHOLOGY, MECHANICAL PROPERTIES AND THERMAL BEHAVIOUR OF POLY(METHYL METHACRYLATE-CO-N-VINYL-2-PYRROLIDONE)/POLY(ETHYLENE GLYCOL)/MULTI-WALLED CARBON NANOTUBES NANOCOMPOSITES

Fang HUANG, Shuaiqian WANG, Mengyao HOU, Zijing DI, Guoqin LIU

College of Material Science and Engineering, Henan University of Technology, Zhengzhou, 450001, China.
Corresponding author:Guoqin LIU, E-mail: guoqin_liu@haut.edu.cn

Abstract. Polymer-based nanocomposites combine increased mechanical properties and heat resistance than pure polymer materials. In this article, poly(methyl methacrylate-co-N-vinyl-2-pyridone)/polyethylene glycol/multi-walled carbon nanotube (P(MMA-co-VP)/PEG/MWCNTs) nanocomposites were prepared by radical copolymerization. To improve the dispersion of MWCNTs in P(MMA-co-VP)/PEG, they were functionalized and characterized with Raman, FTIR spectroscopy, and SEM. The effect of functionalized MWCNTs content on the mechanical and thermal properties of nanocomposites was studied. Although MWCNTs had the potential to induce PEG crystallization, no PEG crystals were found in P(MMA-co-VP)/PEG/MWCNTs. At the same time, MWCNTs had obvious effects as enhancers, and with the increase of their content, the mechanical properties, dynamic modulus and thermal stability of nanocomposites were improved compared with P(MMA-co-VP)/PEG.

Keywords*:* nanocomposites, morphology, mechanical properties, thermal behaviour.

1. INTRODUCTION

The application of poly(methyl methacrylate) (PMMA) in business and industry is self-evident. PMMA is odorless, non-histologically irritating and toxic, insoluble in body fluids, and widely used in biomedicine [1-5]. At the same time, although PMMA can withstand loads and act as a load-bearing component, its own lack of performance limits its wide range of applications. Therefore, in order to expand its application fields, PMMA is modified to improve its performance, among which, the design of PMMA-based composite materials is a commonly used modification method, that is, adding various reinforcing agents, including glass fiber [6, 7], Kevlar fiber [8], TiO_2 [9], multi-walled carbon nanotubes (MWCNTs) [11, 12], SnO_2 [13, 14], etc.

The design of polymer-based nanocomposites has been a research hotspot in recent decades. In nanocomposites, even very low reinforcing agent content (< 2% by volume) may cause positive changes in their properties compared to traditional micron-sized polymer matrix composites, such as radically altering the mechanical and thermal properties of polymer.Among these nanofillers, CNTs are widely used because of their excellent properties [15–18]. CNTs are mainly divided into two categories, namely single-walled carbon nanotubes (SWCNTs) and MWCNTs. Compared to SWCNT, MWCNTs are widely used due to their higher availability, fewer diffusion issues, and lower unit costs.

Poly(N-vinyl-2-pyrrolidone) (PVP) and poly(ethylene glycol) (PEG) are known to be neutral, water-soluble and biocompatible polymer that can often be employed in biotechnology due to their very low cytotoxicity and good biocompatibility with living tissues [19, 20], such as food and additives, cosmetics, coatings as well as in pharmaceutical formulations. Since PVP contains a hydrogen-bonded acceptor-carbonyl group, and PEG contains hydrogen-bonded donor-terminal hydroxyl, therefore, in this study, N-vinyl-2-pyrrolidone (VP) was selected to copolymerize with methyl methacrylate, and the copolymer prepared and PEG can form a stable complex through hydrogen bonding [21].

In the study of related P(MMA-co-VP)/PEG, its morphological and thermal properties have been reported [22], and as a potential biomaterial, its relatively poor mechanical properties and heat resistance limit its application range. In this study, in order to improve the mechanical properties and heat resistance of P(MMA-co-VP)/PEG, P(MMA-co-VP)/PEG/MWCNTs nanocomposites were designed and prepared, that is, MWCNTs were added to P(MMA-co-VP)/PEG. The effects of functionalized MWCNTs content on the morphology, mechanics and thermal properties of nanocomposites were investigated. The process method for the preparation of P(MMA-co-VP)/PEG/MWCNTs nanocomposites by *in-situ* copolymerization is simple, and the prepared nanocomposites are expected to show a wide range of application prospects in bone cement. So far, there have been no reports on the study of P(MMA-co-VP)/PEG/MWCNTs nanocomposites.

2. MATERIALS AND METHODS

2.1. Materials

The purity of the purchased MWCNTs is above 96%. VP and ethylene glycol dimethacrylate (EGDMA) are supplied by Aldrich Chemical Company and used directly. MMA monomers are purified by vacuum distillation prior to use, and 2, 2'-azobisisobutyronitrile (AIBN) is refined by recrystallization in a methanol solution. Before preparing P(MMA-co-VP)/PEG/MWCNTs nanocomposites, PEG (Aldrich) with an average molecular weight of 1000 is heated and dried under vacuum at 75 °C for 6 hours, and PEG can also be used as a dispersant for MWCNTs.

2.2. Synthesis of P(MMA-co-VP)/PEG/MWCNTs nanocomposites

At first, MWCNTs are soaked with mixed acid (H_2SO_4:HNO_3 (v/v)=3:1) and refluxed with them for 6 hr to obtain carboxylic acid functionalized MWCNTs (MWCNTs-COOH). Then, MWCNTs-COOH are washed with deionized water until the pH of the wash water is approximately 7; Subsequently, MWCNTs-COOH are dried in a vacuum oven at 80 °C for 48 hr, and then removed, cooled and dried for later use. Mix MMA (39.1 wt%), VP (26 wt%), PEG (30 wt%) and a certain amount of MWCNTs-COOH (0.50, 1.50, 2.00 and 2.50 wt%, respectively, relative to the total amount of MMA and VP, the same below) and sonicate for 1 hr. AIBN (1.00 wt%) and EGDMA (3.90 wt%) are added to the mixture and ultrasonically dispersed for 40 min while nitrogen gas was bubbled into it. Finally, the mixture is injected into a square mold, and at 50 °C, the polymerization is continued for 24 hr, that is, P(MMA-co-VP)/PEG/MWCNTs nanocomposites are obtained. The vacuum drying of the nanocomposites lasts for 72 hr at 60 °C to remove unreacted monomers.

2.3. Characterization

MWCNTs before and after functionalization and the nanocomposites are characterized by Fourier transform infrared spectroscopy (FTIR, 8300 PCS, Shimadzu) and microconfocal Raman spectroscopy with 633 nm excitation laser (Renishaw 1000 NR), respectively. The nanocomposites' fractured surface is photographed by scanning electron microscope (SEM, JSM-5900LV). Wide-Angle X-Ray Diffraction (WAXD) measurements were performed by Bruker diffractometer (D8 Advance) with Cu Ka radiation. The tensile strength, dynamic mechanical analysis (DMA), and thermogravimetric analysis (TGA) of the nanocomposites were determined on the Instron testing machine (model 4302), DuPont 983 DMA (at 0.1 mm amplitude and N2 atmosphere), and TGA-7 (Perkin-Elmer), respectively.

3. RESULTS AND DISCUSSION

3.1. Characterization of MWCNTs and its nanocomposites

It is believed that, after acid treating MWCNTs, some functional groups could have been covalently linked to CNTs. Raman spectra can be used for judging whether there are some functional groups existed in the surface of MWCNTs. Compared to raw MWCNTs, CNTs treated with mixed acids show a significant increase in their disorder band (D-band) intensity in their Raman spectra, as shown in Fig. 1. The strong acid

treatment of MWCNTs leads to an increase in their structural defects, mainly due to the oxidation fragments covering their surface after acid handling, which form carboxylic acid groups [23], namely carboxylic acid functionalized MWCNTs (MWCNTs-COOH).

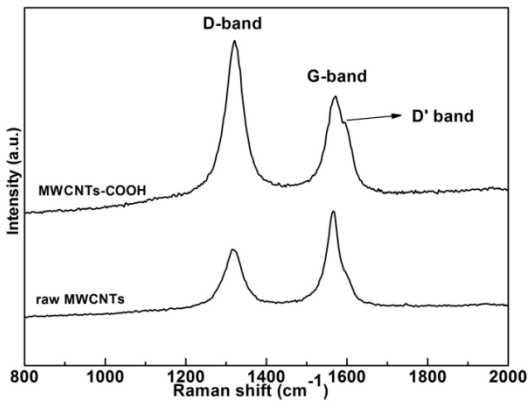

Fig. 1 – Raman spectra of raw and acid-treated MWCNTs.

In Fig. 1, the G-band and D-band appear around 1 572 and 1 320 cm^{-1}, respectively, corresponding to tangential and disordered mode. In fact, in the Raman spectra of CNTs, the intensity ratio (I_D/I_G) of the D-band to the G-band can often be used to characterize the degree of surface defects, and the larger the I_D/I_G value, the more structural defects there are. The I_D/I_G of raw MWCNTs is 0.80, however, that of MWCNTs-COOH is 1.18, which is due to the oxidation of the uniform surface of raw MWCNTs after acid treatment, damaging the wall of CNTs to a certain extent and forming carboxylic acid groups. Meanwhile, a shoulder peak called the D'-band appears at 1 593 cm^{-1} in the G-band of MWCNTs-COOH, while no shoulder peak in the D'-band is observed in the G-band of raw MWCNTs. The D'-band, like the D-band, is caused by disorder and defects, again indicating that the number of defects on MWCNTs increases after mixed acid treatment.

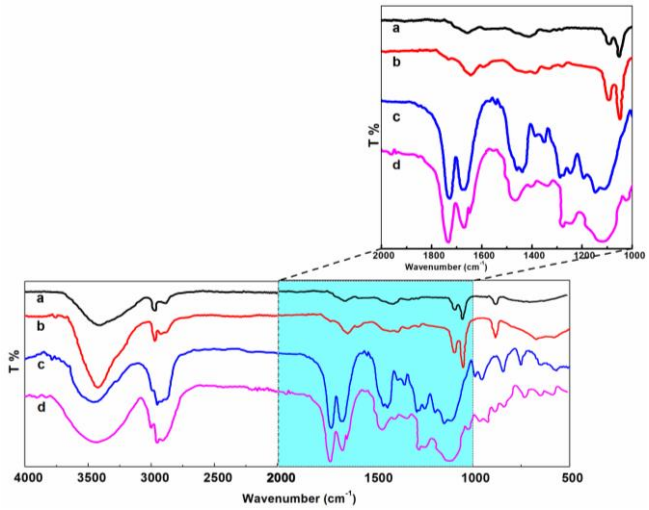

Fig. 2 – FTIR spectra of raw MWCNTs (a), MWCNTs-COOH (b), P(MMA-co-VP)/PEG (c) and P(MMA-co-VP)/PEG/2.5 wt% MWCNTs (d).

In their FTIR, the changes in the absorption wavelengths of the corresponding functional groups of MWCNTs, MWCNTs-COOH, P(MMA-co-VP)/PEG and their composite materials can be used to characterize their interactions. Figure 2 shows FTIR of the raw MWCNTs, MWCNTs-COOH, P(MMA-co-VP)/PEG and their nanocomposites. Firstly, comparing the FTIR of the original MWCNTs and MWCNTs-COOH (Fig. 2a and b), MWCNTs-COOH shows obvious absorption peaks at 1 734 cm^{-1}, corresponding to the carbonyl (-C=O) tensile vibration generated by its mixed acid treatment; about 3 425 cm^{-1}, there is a stronger absorption peak caused by hydroxyl (-OH) tensile vibration; therefore, it can be concluded that MWCNTs are oxidized by mixed acids to produce -COOH on their surface.

It has been reported that there is a hydrogen bond between the carbonyl group of PVP and the hydroxyl group of PEG [22]. In P(MMA-co-VP)/PEG/MWCNTs, due to the presence of -COOH on the surface of MWCNTs treated with mixed acid, hydrogen bonds may form between MWCNTs-COOH and P(MMA-co-VP)/PEG. Therefore, in this study, the infrared absorption peaks of -OH and -COOH are focused on.

In FTIR of P(MMA-co-VP)/PEG and MWCNTs-COOH, the broadband centered on 3463 and 3 422 cm^{-1} is their -OH vibration absorption peak, respectively, as shown in Fig. 2b and c; the vibrations of -OH in P(MMA-co-VP)/PEG/MWCNTs appear as a broadband centered at 3 444 cm^{-1}, as shown in Fig. 2d, which could be attributed to the interaction between -OH and different functional groups. Another point of interest is the -C=O vibration region of P(MMA-co-VP)/PEG. There are two -C=O vibration peaks observed at around 1 670 and 1 727cm^{-1}, corresponding to -C=O of PVP and PMMA. In FTIR of P(MMA-co-VP)/PEG/MWCNTs, the -C=O peak of PVP at 1 666 cm^{-1} corresponds to the free -C=O. Additionally, a shoulder peak at 1 649 cm^{-1}, which is redshifted due to hydrogen bond formation, can be observed near it. On the other hand, the wavenumber of -C=O of PMMA shows almost no change, indicating that the -C=O of PMMA does not participate in the formation of hydrogen bonds. It may be deduced that hydrogen bonds are exclusively formed between the -OH of MWCNTs-COOH and the -C=O of PVP, but not between MWCNTs-COOH and PMMA.

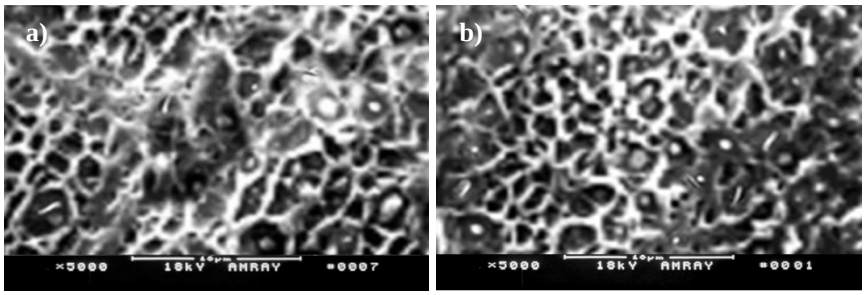

Fig. 3 – SEM images of P(MMA-co-VP)/PEG/MWCNTs nanocomposites with 0.5 wt% (a)) and 2.5 wt% MWCNTs (b)).

The key to the successful preparation of P(MMA-co-VP)/PEG/MWCNTs nanocomposites is to solve the problem of uniform dispersion of nanoparticles in the polymer matrix, so that MWCNTs can play a reinforcing role. Figure 3 are SEM images of the fracture surface of P(MMA-co-VP)/PEG/MWCNTs composites containing 0.5 and 2.5 wt% MWCNTs, respectively. It can be seen MWCNTs are evenly distributed in the P(MMA-co-VP)/PEG networks and do not form their aggregates.

These can be attributed to the hydrogen bonding between acid treated MWCNTs and P(MMA-co-VP)/PEG networks, as shown in previous infrared spectroscopy analysis, which promotes the dispersion of MWCNTs in the polymer and avoids the formation of MWCNTs' aggregates. At the same time, the hydrogen bonds present at the interface between the polymer and MWCNTs can play a physical cross-linking role, which is also beneficial for improving the mechanical properties of the polymer.

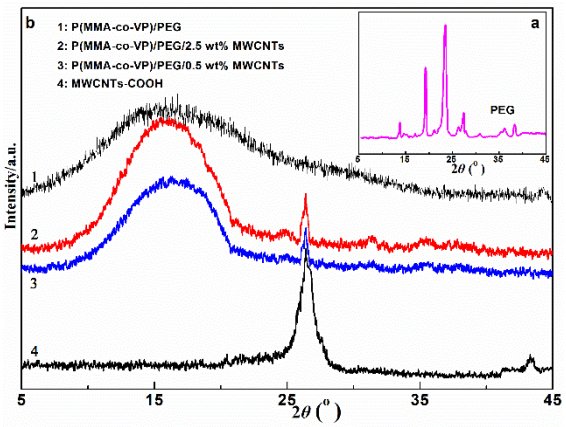

Fig. 4 – WAXD of PEG (a), P(MMA-co-VP)/PEG, the nanocomposites and MWCNTs-COOH (b).

It has been reported that, although PEG has a crystalline structure, due to the hydrogen bonding between PEG and the P(MMA-co-VP) networks, their blends are completely amorphous [22]. On the other hand, there are reports that MWCNTs can induce crystallization [24, 25]. It is worth paying attention to whether MWCNTs can induce PEG crystallization in P(MMA-co-VP)/PEG/MWCNTs, because the crystallization phase has a certain effect on the properties of the material.

Figure 4 is WAXD of PEG, MWCNTs, P(MMA-co-VP)/PEG and their nanocomposites. For pure PEG, in Fig. 4a, at 2θ angles of 19.2° and 23.4°, there are diffraction peaks corresponding to the (120) and (132) crystal planes of the PEG monoclinic system, respectively [26]. In Fig. 4b, P(MMA-co-VP)/PEG shows a wider diffraction peak compared to pure PEG, while the two characteristic diffraction peaks of pure PEG are not shown in it, indicating that it is amorphous and the crystal structure of PEG is significantly destroyed due to the hydrogen bonding interaction between P(MMA-co-VP) and PEG. At the same time, MWCNTs-COOH have diffraction peaks at 2θ of 26.4° and 43.2°, corresponding to the (002) and (100) crystal planes of the hexagonal graphite structure, respectively [27]. Although MWCNTs have the effect of inducing crystal crystallization, in P(MMA-co-VP)/PEG/MWCNTs nanocomposites, the characteristic diffraction peaks associated with PEG crystals disappear, and only the diffraction peak of MWCNTs is observed at 2θ of 26.4°. In other words, the incorporation of MWCNTs into P(MMA-co-VP)/PEG to form nanocomposites does not induce the crystallization of PEG crystals.

3.2. Mechanical properties

To improve the mechanical properties of polymers by incorporating MWCNTs, it is necessary to solve the effective transfer of load between them and MWCNTs. If there is weak or no interfacial adhesion between the two phases, MWCNTs exhibit hole or nanostructure defects, leading to local stress concentration and loss of MWCNTs' ability to enhance the polymer. In order to investigate the effect of MWCNTs incorporation on the mechanical properties of polymers, the mechanical properties of P (MMA-co-VP)/PEG/MWCNTs nanocomposites are tested.

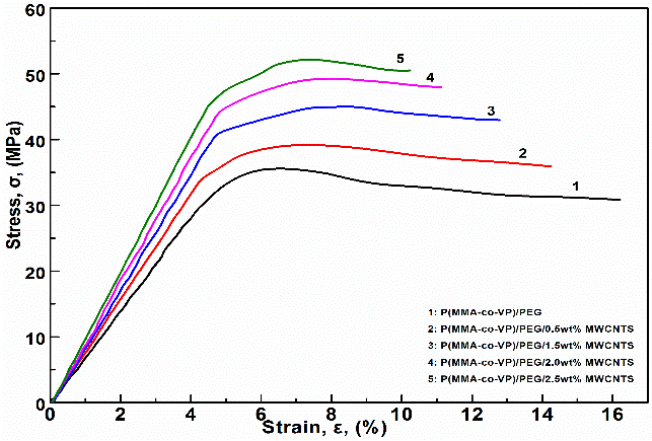

Fig. 5 – Stress–strain curves of P(MMA-co-VP)/PEG and the nanocomposites.

The stress (σ) – strain (ε) curves of P(MMA-co-VP)/PEG and its nanocomposites with different MWCNTs weight fractions are shown in Fig. 5. Firstly, by comparing their maximum tensile strength (σ_{max}), the changes in its strength are studied. The σ_{max} of P(MMA-co-VP)/PEG is about 35.6 MPa, while that of the nanocomposites with 0.5, 1.5, 2.0 and 2.5 wt % of MWCNTs are 39.2, 45.1, 49.3 and 52.2 MPa separately, which increase by 10, 27, 38 and 47% in comparison of P(MMA-co-VP)/PEG, respectively.

At same time, in Fig. 6, the Young's modulus of P(MMA-co-VP)/PEG is around 0.71 GPa, while that of the nanocomposites with 0.5, 1.5, 2.0 and 2.5 wt % of MWCNTs are 0.79, 0.87, 0.93 and 1.0 GPa separately, which increase by 11, 23, 31 and 41% in comparison of P(MMA-co-VP)/PEG, respectively.

In conclusion, in P (MMA-co-VP)/PEG/MWCNTs nanocomposites, their tensile strength and Young's modulus increase with the increase of MWCNTs loading, indicating that MWCNTs effectively enhance the mechanical properties of the polymers. This also indirectly proves that MWCNTs are effectively dispersed in P(MMA-co-VP)/PEG, and their interfacial hydrogen bonding can effectively transfer the load between them.

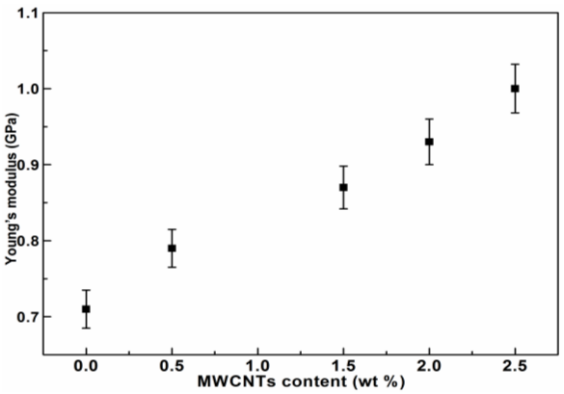

Fig. 6 – Young's modulus of P(MMA-co-VP)/PEG and the nanocomposites.

3.3. Thermal analysis

The incorporation of MWCNTs into polymer should enhance thermal properties, such as dynamic mechanical properties and thermal stability. Polymer is a kind of viscoelastic material that combines the properties of a viscous liquid and an elastic solid. Figure 7a and b shows the curves of the storage modulus (E') and loss tangent (tanδ) of P(MMA-co-VP)/PEG and its nanocomposites *vs.* temperature, respectively. E' denotes the stiffness of the viscoelastic material, tanδ reflects the energy lost in heat due to intramolecular friction, and the temperature of the maximum tanδ is generally defined as the glass transition temperature (T_g).

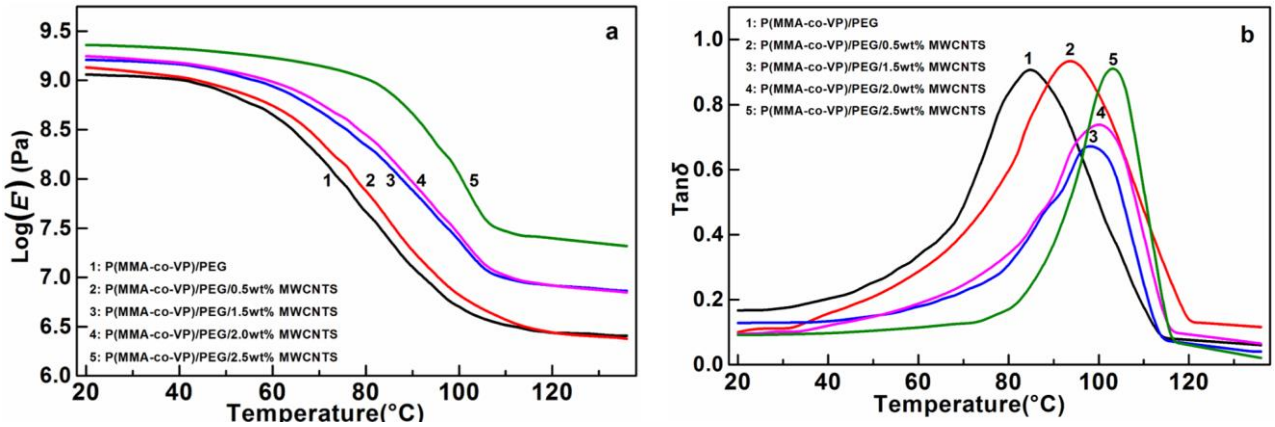

Fig. 7 – E' (a) and tanδ (b) of P(MMA-co-VP)/PEG and its nanocomposites.

In Fig. 7a, it can be seen that due to the excellent mechanical properties of CNTs, compared with P (MMA-co-VP)/PEG, the incorporation of MWCNTs significantly improves the E' of the nanocomposite and the initial modulus increases with the increase of MWCNTs loading. In Fig. 7b, P(MMA-co-VP)/PEG and its nanocomposites only show a single tanδ peak, indicating they are completely homogeneous glass phase without phase separation, which is consistent with WAXD analysis. In addition, with the increase of MWCNTs loading, the tanδ peak of the nanocomposites shifted to high temperature. Generally, tanδ is related to the strain energy of viscous friction loss, and a higher tanδ value indicates polymers tend to have viscosity rather than elasticity. On the other hand, since the temperature corresponding to the peak of the tanδ curve is considered T_g, the T_g of the nanocomposites increases by at least 9 °C compared to that of P(MMA-co-VP)/PEG.

In summary, the incorporation of MWCNTs into P(MMA-co-VP)/PEG shows an increase in E', and tanδ of their nanocomposites, which can be attributed to the decrease in the free space for polymer molecular vibration due to the influence of nanoscale MWCNTs. Well-dispersed MWCNTs generate large interfacial regions that can limit the behavior of the surrounding polymeric matrix, resulting in a co-continuous network of significantly changed polymeric chain motion. At the same time, MWCNTs can be used as physical crosslinkers to partially limit the molecular motion of polymers and improve the stiffness of the nanocomposites.

By adding CNTs, the thermal stability of polymeric nanocomposites can be significantly improved, which can be attributed to the high thermal conductivity and heat flow blocking effect of CNTs. TGA thermograms of MWCNTs, P(MMA-co-VP)/PEG and their nanocomposites are shown in Fig. 8.

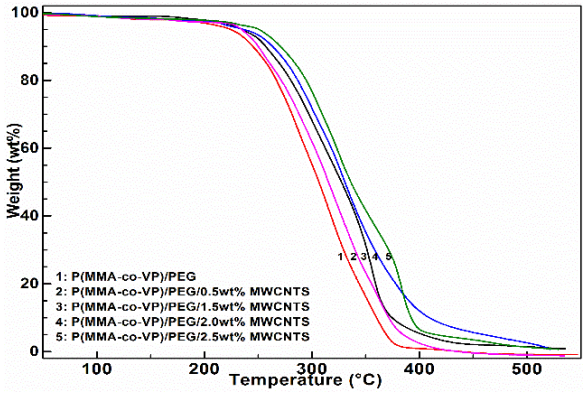

Fig. 8 – TGA curves of P(MMA-co-VP)/PEG and its nanocomposites.

In Fig. 8, here, the temperature corresponding to 5% weight loss is identified as the thermal degradation temperature (T_d). Comparing the T_d of the nanocomposite material with that of P(MMA-co-VP)/PEG, it can be found that the Td of the nanocomposite material is at least 12 °C higher; it can be observed that at 358 °C, the weight loss rate of nanocomposites is between 60 and 79%, while that of P(MMA-co-VP)/PEG is about 85%. These results suggest that the incorporation of MWCNTs can improve the thermal stability of polymers, which may be caused by the following factors: a) the high thermal conductivity of CNTs promotes heat consumption [28]; b) CNTs, as electron acceptors, can capture high-energy free radicals during thermal degradation [29]. c) The interaction between CNTs and polymers plays a role in physical cross-linking.

4. CONCLUSIONS

Due to the hydrogen bonding between the acid-treated MWCNTs and PVP, the MWCNTs were uniformly dispersed in P(MMA-co-VP)/PEG without their any aggregates. Although MWCNTs have the effect of inducing crystallization, the crystallization of PEG in nanocomposites is not observed. Compared with P(MMA-co-VP)/PEG, the tensile strength and Young's modulus of the nanocomposites increased with the increase of MWCNTs content, and their tensile strength and Young's modulus increased by up to 47 % and 41 %, respectively. At the same time, the glass state modulus of nanocomposites increases with the increase of MWCNTs loading. The incorporation of MWCNTs into P(MMA-co-VP) significantly increased the T_g of nanocomposites by more than 9 °C, and improved the thermal stability of P(MMA-co-VP)/PEG.

ACKNOWLEDGMENTS

This work was supported by the Science and Technology Project of Henan Province (No. 172102210033).

REFERENCES

[1] Yanıkoğlu ND, Sakarya RE. Test methods used in the evaluation of the structure features of the restorative materials: a literature review. Journal of Materials Research and Technology 2020;9:9720–9734.
[2] Díez-Pascual AM. PMMA-based nanocomposites for odontology applications: a state-of-the-art. International Journal of Molecular Sciences 2022;23:10288.
[3] D'Elia A, Deering J, Clifford A, Lee BEJ, Grandfield K, Zhitomirsky I. Electrophoretic deposition of polymethylmethacrylate and composites for biomedical applications. Colloids and Surfaces B: Biointerfaces 2020;188:110763.
[4] T. G. Xu, D. C. Liu, Y. Wang, S. Chen, B. Li, F. Zhang, & J. H. He, Tungsten carbide-enhanced radiopaque and biocompatible PMMA bone cement and its application in vertebroplasty, Composites Communications, 40, pp. 101615, 2023.

[5] Boschetto F, Honma T, Adachi T, Kanamura N, Zhu W, Yamamoto T, Marin E, Pezzotti G. Development and evaluation of osteogenic PMMA bone cement composite incorporating curcumin for bone repairing. Materials Today Chemistry 2023; 27:101307.
[6] Mackin CD, Saha GC. Design, pultrusion manufacturing, characterization, and reliability testing of a novel PMMA-based glass FRP composite material. Transportation Engineering 2022;8:100108.
[7] Belkheir M, Rouissat M, Mokaddem A, Doumi B, Boutaous A. Using genetic algorithm for studying the effect of Polymethyl methacrylate (PMMA) polymer matrix on composites materials interface based on carbon, glass and aramid fibers for engineering and telecommunication applications. Computational Particle Mechanics 2023;10:405–414.
[8] Yerliyurt K, Taşdelen TB, Eğri Ö, Eğri S. Flexural properties of heat-polymerized PMMA denture base resins reinforced with fibers with different characteristics. Polymers 2023;15:3211.
[9] Darwish G, Huang S, Knoernschild K, Sukotjo C, Campbell S, Bishal AK, Barão VA, Wu CD, Taukodis CG, Yang B. Improving polymethyl methacrylate resin using a novel titanium dioxide coating. Journal of Prosthodontics 2019;28:1011–1017.
[10] Chelu M, Stroescu H, Anastasescu M, Calderon-Moreno JM, Preda S, Stoica M, Fogarassy Z, Petrik P, Gheorghe M, Parvulescu C, Brasoveanu C. High-quality PMMA/ZnO NWs piezoelectric coating on rigid and flexible metallic substrates. Applied Surface Science 2020;529:147135.
[11] Ameen Khan M, Madhu GM, Sailaja RRN. Polymethyl methacrylate reinforced with nickel coated multi-walled carbon nanotubes: Flame, electrical and mechanical properties. Polymer Composites 2021;42:498–511.
[12] Zhang H, Zhong J, Zhang X, Shi X, Yang L, Sun S, Zuo M, Song Y, Zheng Q. Controlling the enrichment location of brush grafted multi-walled carbon nanotubes at the interface of various polymer blends. Polymer 2022;238:124427.
[13] Pethaperumal S, Mohanraj GT. Green synthesis, characterization of SnO_2 3D microbars with surface 2D nanostructures and evaluation of electrical properties of PMMA-SnO_2 hybrid nanocomposites. Surfaces and Interfaces 2022;34:102381.
[14] Ćelić N, Banić N, Jagodić I, Yatskiv R, Vaniš J, Štrbac G, Lukić-Petrović S. Eco-friendly photoactive foils based on ZnO/SnO_2-PMMA nanocomposites with high reuse potential. ACS Applied Polymer Materials 2023;5:3792–3800.
[15] Zhang X, Lu W, Zhou G, Li Q. Understanding the mechanical and conductive properties of carbon nanotube fibers for smart electronics. Advanced Materials 2020;32:1902028.
[16] Abazari S, Shamsipur A, Bakhsheshi-Rad HR, Ismail AF, Sharif S, Razzaghi M, Ramakrishna S, Berto F. Carbon nanotubes (CNTs)-reinforced magnesium-based matrix composites: A comprehensive review. Materials 2020;13:4421.
[17] Liang X, Li H, Dou J, Wang Q, He W, Wang C, Li D, Lin JM, Zhang Y. Stable and biocompatible carbon nanotube ink mediated by silk protein for printed electronics. Advanced Materials 2020;32:2000165.
[18] Han W, Zhou J, Shi Q. Research progress on enhancement mechanism and mechanical properties of FRP composites reinforced with graphene and carbon nanotubes. Alexandria Engineering Journal 2023;64:541-579.
[19] Ma L, Liu M, Chen J, Liu H, Cui D, Gao C. Synthesis, characterization and drug release behavior of pH-responsive O-carboxymethyl chitosan-graft-poly (N-vinylpyrrolidone) hydrogel beads. Advanced Engineering Materials 2009;11; B267–B274.
[20] Yiğitoğlu M, Işıklan N, Özmen R. Graft copolymerization of N-vinyl-2-pyrrolidone onto sodium carboxymethylcellulose with azobisisobutyronitrile as the initiator. Journal of Applied Polymer Science 2007;104:936–943.
[21] Sengwa RJ. Microwave dielectric relaxation and molecular dynamics in binary mixtures of poly (vinyl pyrrolidone)-poly (ethylene glycol) s in non-polar solvent, Polymer International 2003;52:1462–1467.
[22] Liu G, Liu Z, Zou W, Li Z, Peng J, Cheng W, Xu S. Morphology and thermal behaviour of poly (methyl methacrylate-co–N-vinyl-2-pyrrolidone) /poly (ethylene glycol) semi-interpenetrating polymer networks based on hydrogen bonding interaction. Acta Chimica Slovenica 2009;56:946–952.
[23] Hu H, Zhao B, Itkis ME, Haddon RC. Nitric acid purification of single-walled carbon nanotubes. The Journal of Physical Chemistry B 2003;107:13838–13842.
[24] Pandey P, Mohanty S, Nayak SK. Tailoring dispersion and interaction of MWNT in polymer nanocomposites, using Triton X-100 as nonionic surfactant, Journal of Materials Engineering and Performance 2014;23:4385–4393.
[25] Perez RA, Lopez JV, Hoskins JN, Zhang B, Grayson SM, Casas MT, Puiggalí J, Müller AJ. Nucleation and antinucleation effects of functionalized carbon nanotubes on cyclic and linear poly (ε-caprolactones). Macromolecules 2014;47: 3553–3566.
[26] Takahashi Y, Tadokoro H. Structural studies of polyethers, $(-(CH_2)_mO-)_n$. X. Crystal structure of poly (ethylene oxide). Macromolecules 1973;6:672–675.
[27] Li W, Liang C, Zhou W, Qiu J, Zhou Z, Sun G, Xin Q. Preparation and characterization of multiwalled carbon nanotube-supported platinum for cathode catalysts of direct methanol fuel cells. The Journal of Physical Chemistry B 2003;107: 6292–6299.
[28] Ge JJ, Hou H, Li Q, Graham MJ, Greiner A, Reneker DH, Harris FW, Cheng SZ. Assembly of well-aligned multiwalled carbon nanotubes in confined polyacrylonitrile environments: electrospun composite nanofiber sheets. Journal of the American Chemical Society 2004;126:15754–15761.
[29] Watts PCP, Fearon PK, Hsu WK, Billingham NC, Kroto HW, Walton DRM. Carbon nanotubes as polymer antioxidants. Journal of Materials Chemistry 2003;13:491–495.

Received December 20, 2023